Electronic Supplementary Material (ESI) for Journal of Materials Chemistry A.

Supporting Information

Self-healing, deformation-resistant MXene double-network hydrogel for stable solar-driven interfacial evaporation

Ruiqi Zhao, [a] Xushuai Chen, [a] Xi Chen, * [a] Panpan Zhan, [a] Chunjia Luo, [a] Pengfei Zhang, * [b] Min Chao, [a] Luke Yan, *[a]

a. School of Materials Science & Engineering, Chang'an University, Xi'an, 710064, China. E-mail: yanlk_79@hotmail.com
b. School of Textile Science and Engineering, Xi'an Polytechnic University, Xi'an, 710048, China. E-mail: fengyunjian1981@126.com

Note S1 Salt rejection performance.

To quantify the salt repellency of DN-CA/PAAm hydrogels, 20 wt% of DN-CA/PAAm hydrogels were first dried in an oven for 24 h to a mass of m_1, and then the hydrogels were soaked in a 3.5 wt.% NaCl solution for 24 h to allow for full swelling. The fully swollen hydrogel (m_2) was then dried again in an oven for 24 h to obtain a hydrogel of mass m_3, which includes the dry mass of the hydrogel (m_1) and the salt infiltrated into the gel. The salt removal rate φ is given by Equation (1)[S1]:

$$\varphi = 1 - \frac{m_3 - m_1}{0.035 \times (m_2 - m_1)} \quad (1)$$

Note S2 Dehydration/rehydration stability.

To quantify the dehydration/rehydration stability of the hydrogels, the hydrogels were first dried in an oven for 12 h to obtain a hydrogel with mass m_0, and then soaked in DI water for 12 h. Then the hydrogel was subjected to dehydration/rehydration cycles, the hydrogel after each dehydration cycle with mass u, and the hydrogel after each rehydration cycle with mass n. The water content w is given by Equation (2):

$$w = \frac{n - u}{m_0} \quad (2)$$

Supplementary Figures

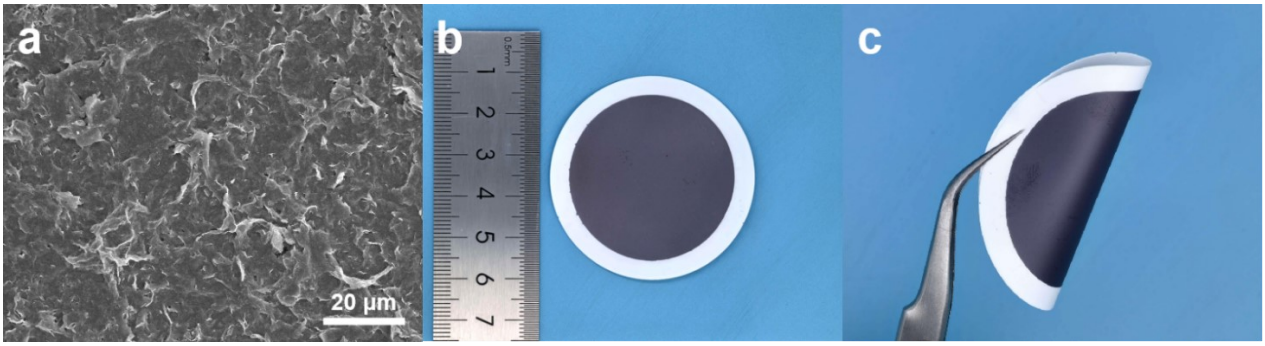

Figure S1 (a) Surface SEM image of MXene film. (b), (c) Photos of MXene film.

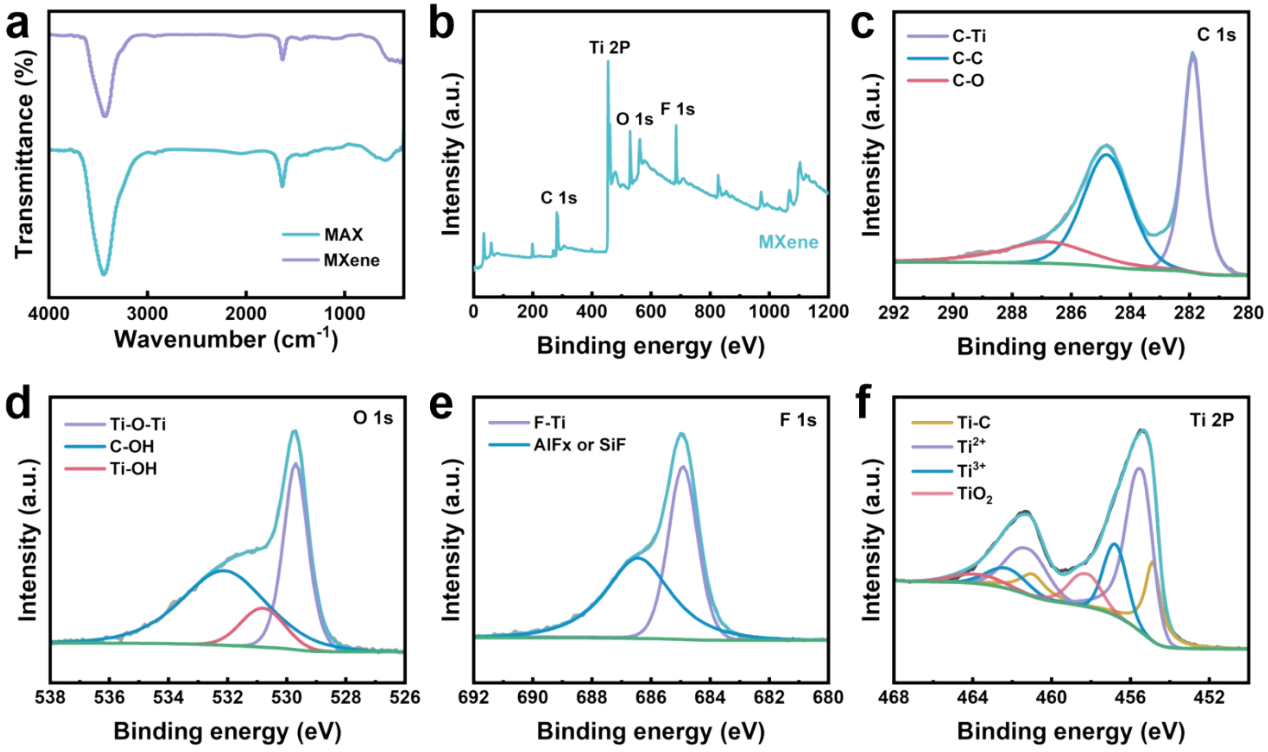

Figure S2 (a) FTIR spectra of MXene film. (b) XPS survey of the MXene. High-resolution XPS for (c) C 1s, (d) O 1s, (e) F 1s and (f) Ti 2p.

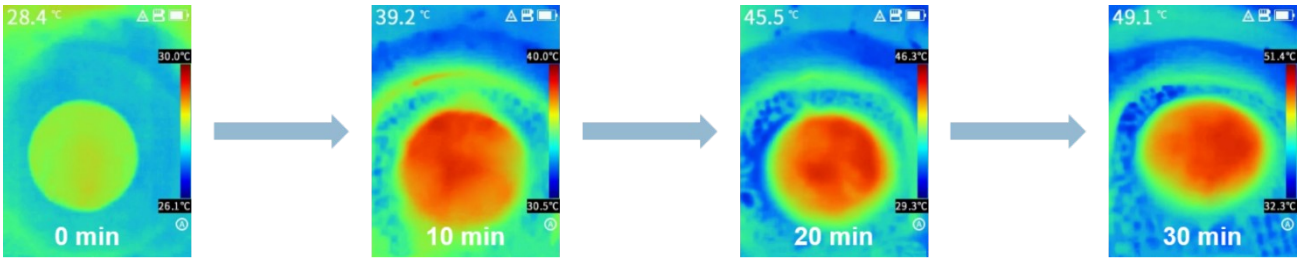

Figure S3 0 - 30 min infrared image of MXene film under 1 sun.

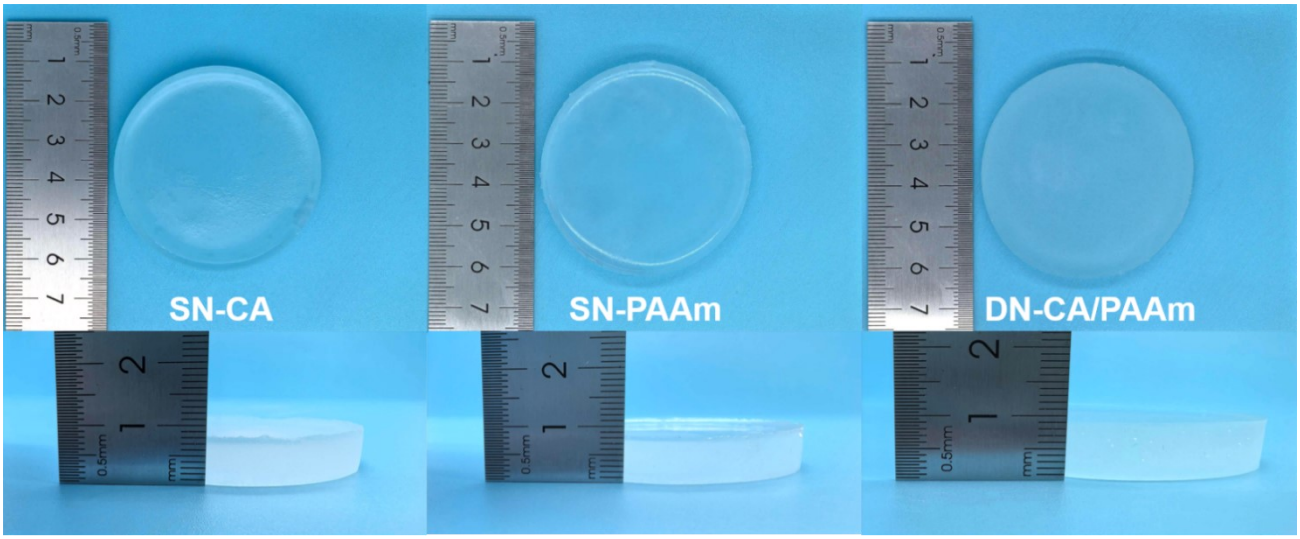

Figure S4 Photos of SN-CA, SN-PAAm and DN-CA/PAAm hydrogels.

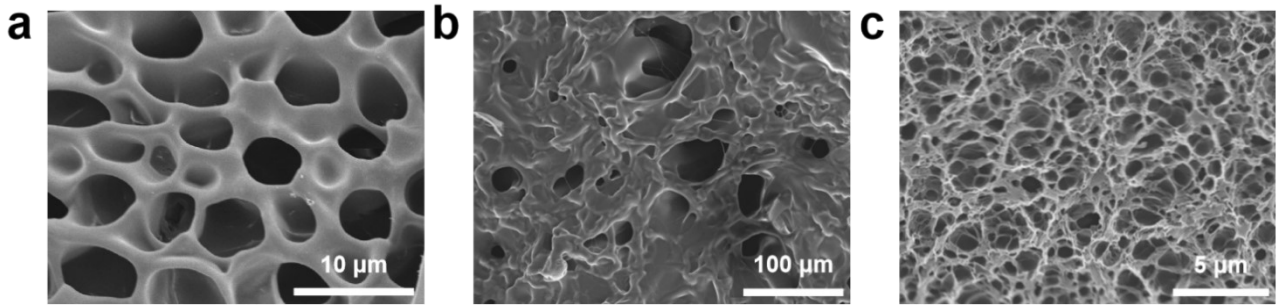

Figure S5 Surface SEM image of (a) DN-CA/PAAm、(b) SN-CA and (c) SN-PAAm hydrogels.

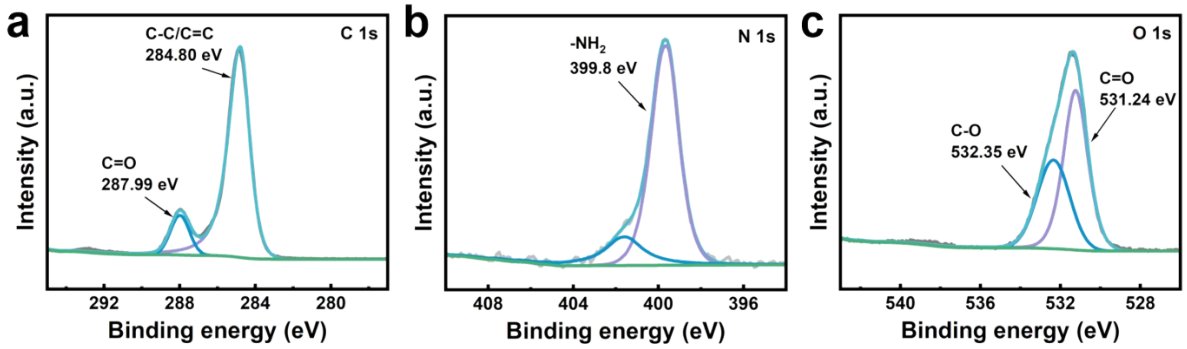

Figure S6 XPS for DN-CA/PAAm hydrogel in the (a) C 1s region, (b) N 1s region, (c) O 1s region.

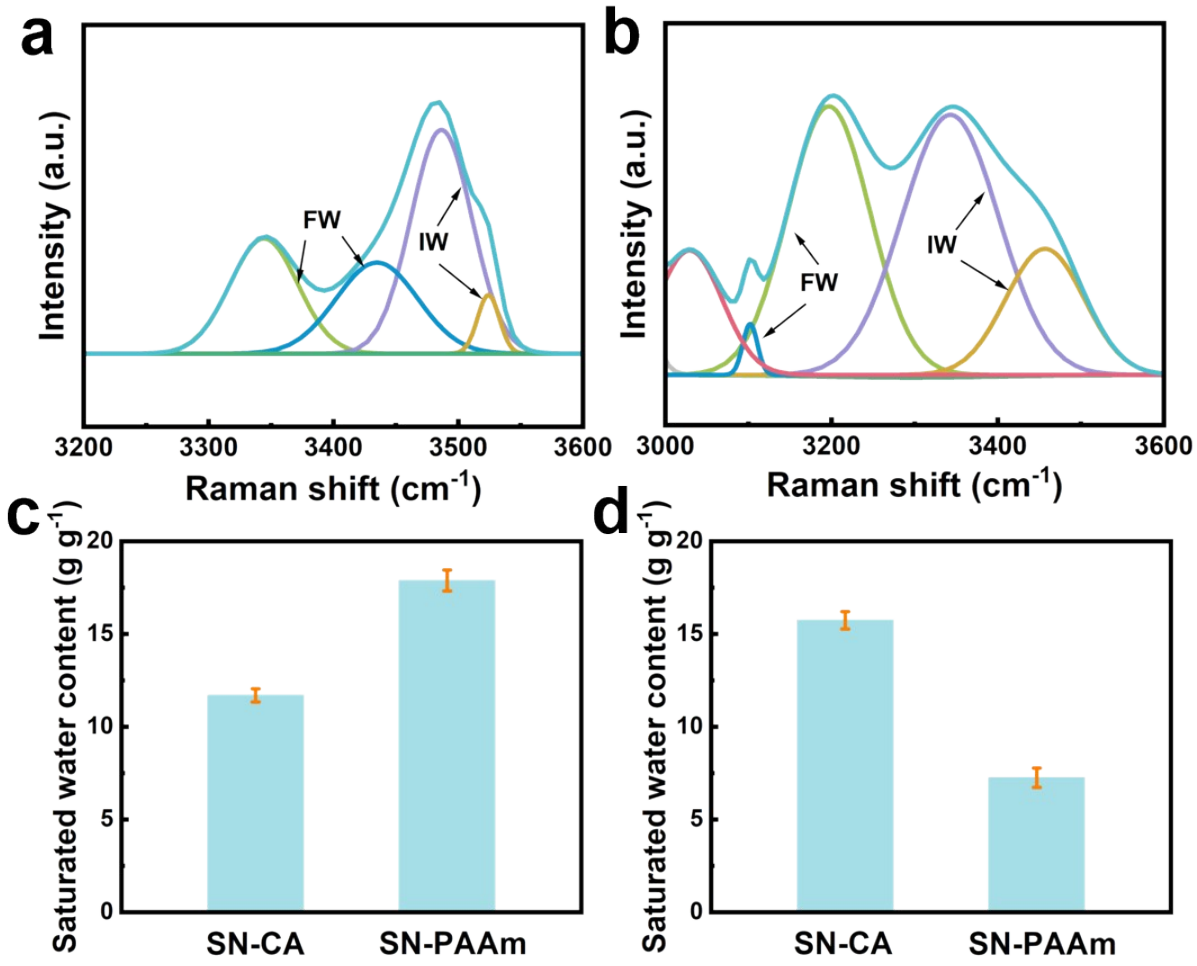

Figure S7 Raman survey of (a) SN-CA and (b) SN-PAAm hydrogel samples. Saturated water content of SN-CA and SN-PAAm hydrogels in (c) DI water and (d) 3.5 wt% NaCl solution.

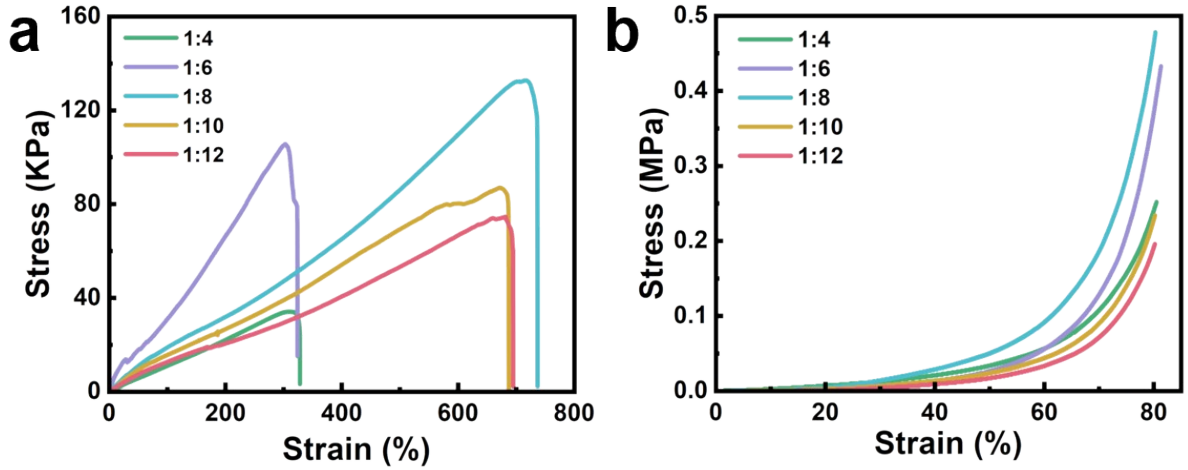

Figure S8 (a) Tensile strength and (b) Compressive strength of different ratios of DN-CA/PAAm hydrogels.

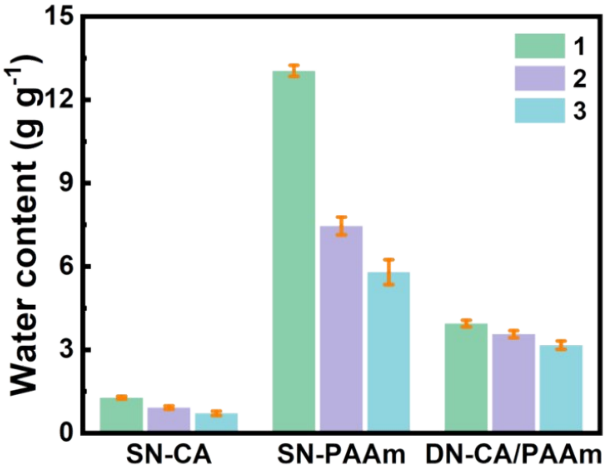

Figure S9 Water content of SN-CA, SN-PAAm and DN-CA/PAAm hydrogels in simulated seawater.

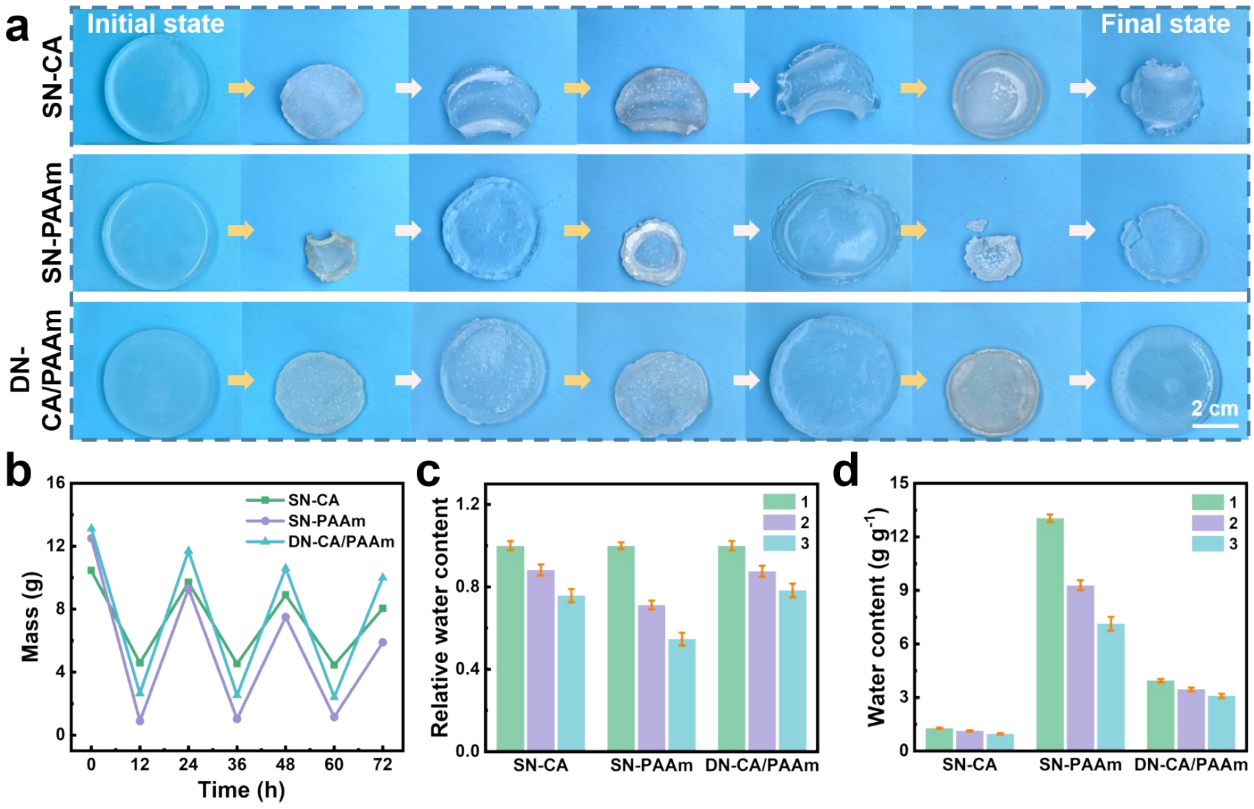

Figure S10 (a) Photographs of hydrogels dehydration/rehydration cycles in simulated seawater. (b) Mass and (c) Water content of SN-CA, SN-PAAm and DN-CA/PAAm hydrogels. (d) Water content of SN-CA, SN-PAAm and DN-CA/PAAm hydrogels.

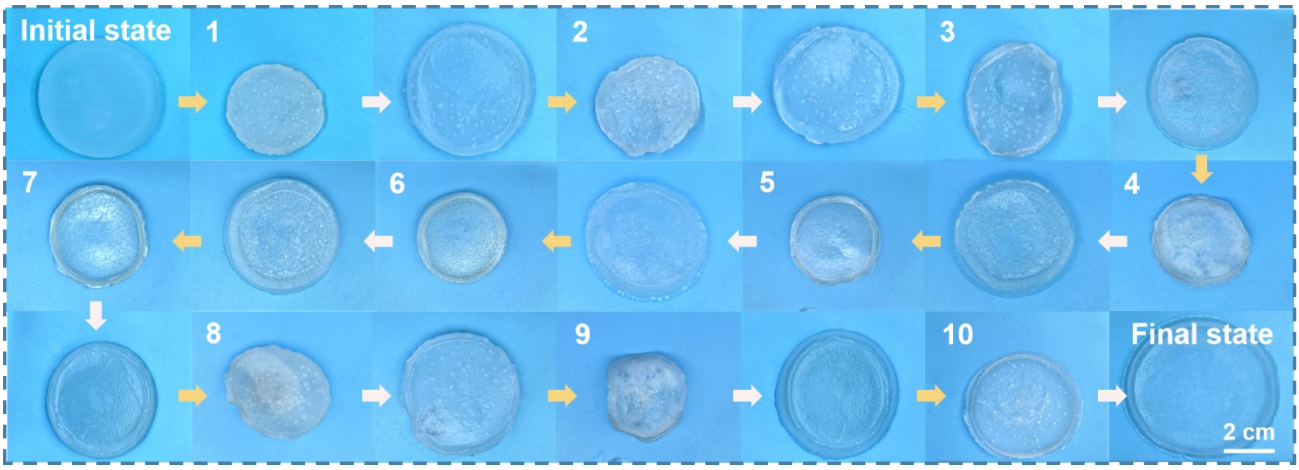

Figure S11 Photographs of DN-CA/PAAm hydrogels dehydration/rehydration cycles in DI water.

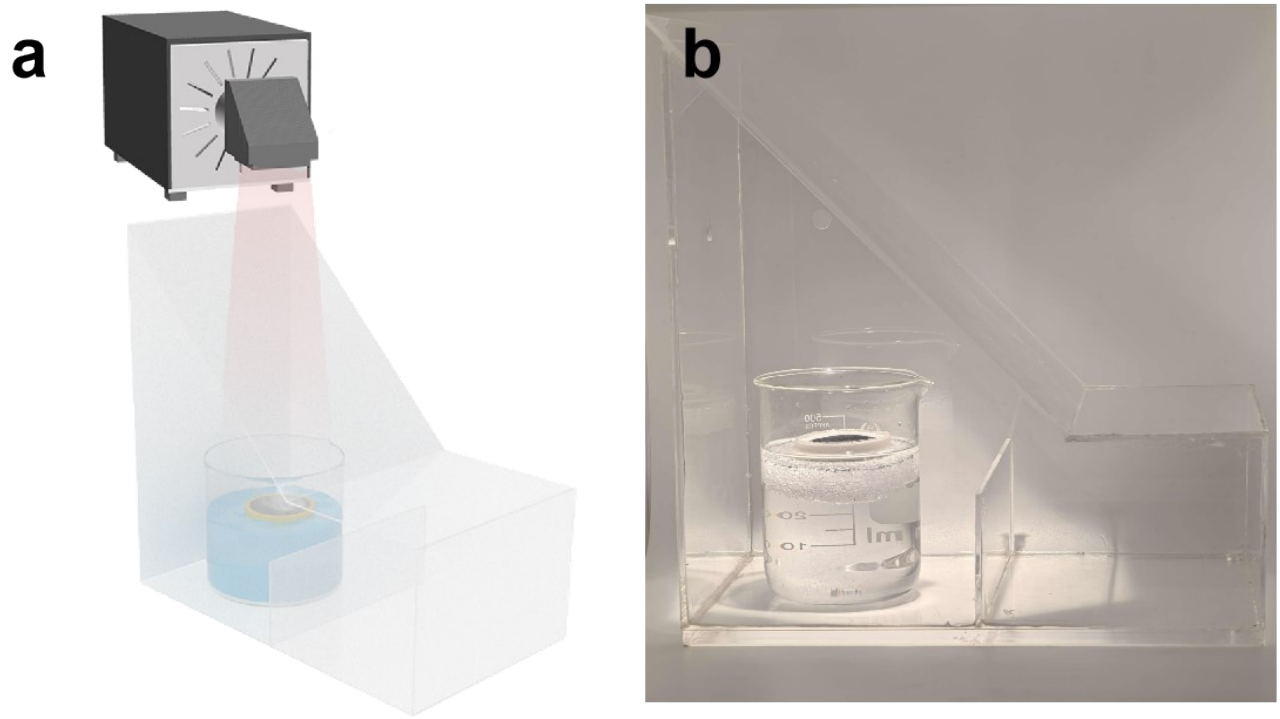

Figure S12 (a) Schematic diagram of the MCPH evaporator. (b) Photograph of MCPH photothermal evaporator setup.

During the experiments, a layer of MXene membrane with a photothermal area of 12.56 cm^2 was placed on the surface of the DN-CA/PAAm hydrogel to form the evaporator, which was operated on a support foam.

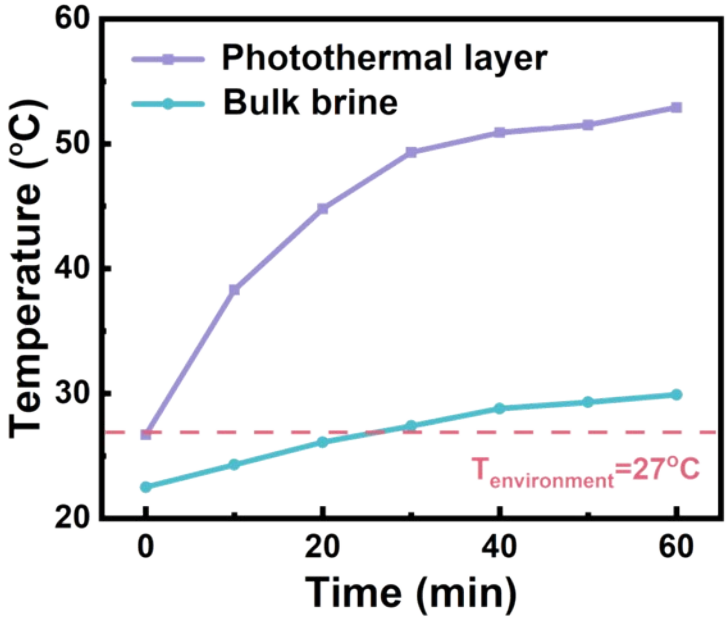

Figure S13 Temperature curves of MCPH evaporator and bulk water under 1 sun for 0 - 60 min.

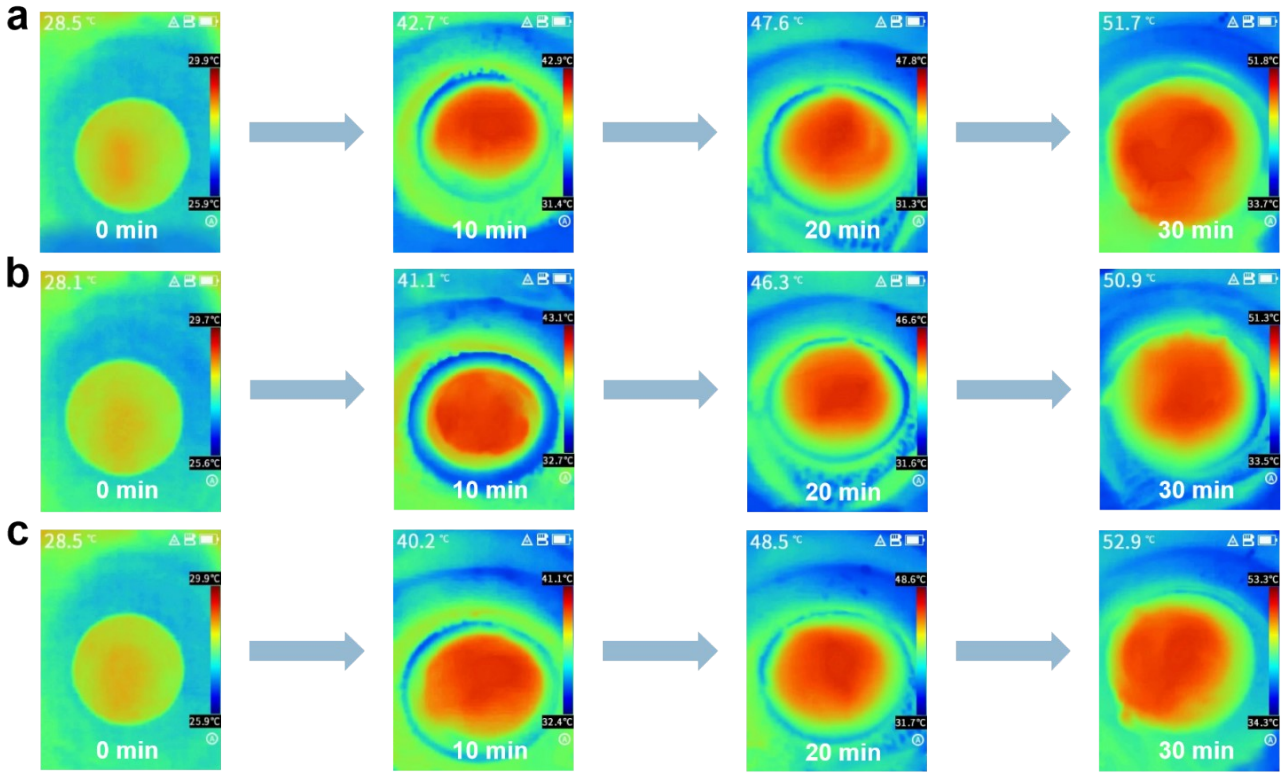

Figure S14 Infrared thermal image of (a) MCH, (b) MPH and (c) MCPH vaporizer under 1 sun for 0 - 30 min.

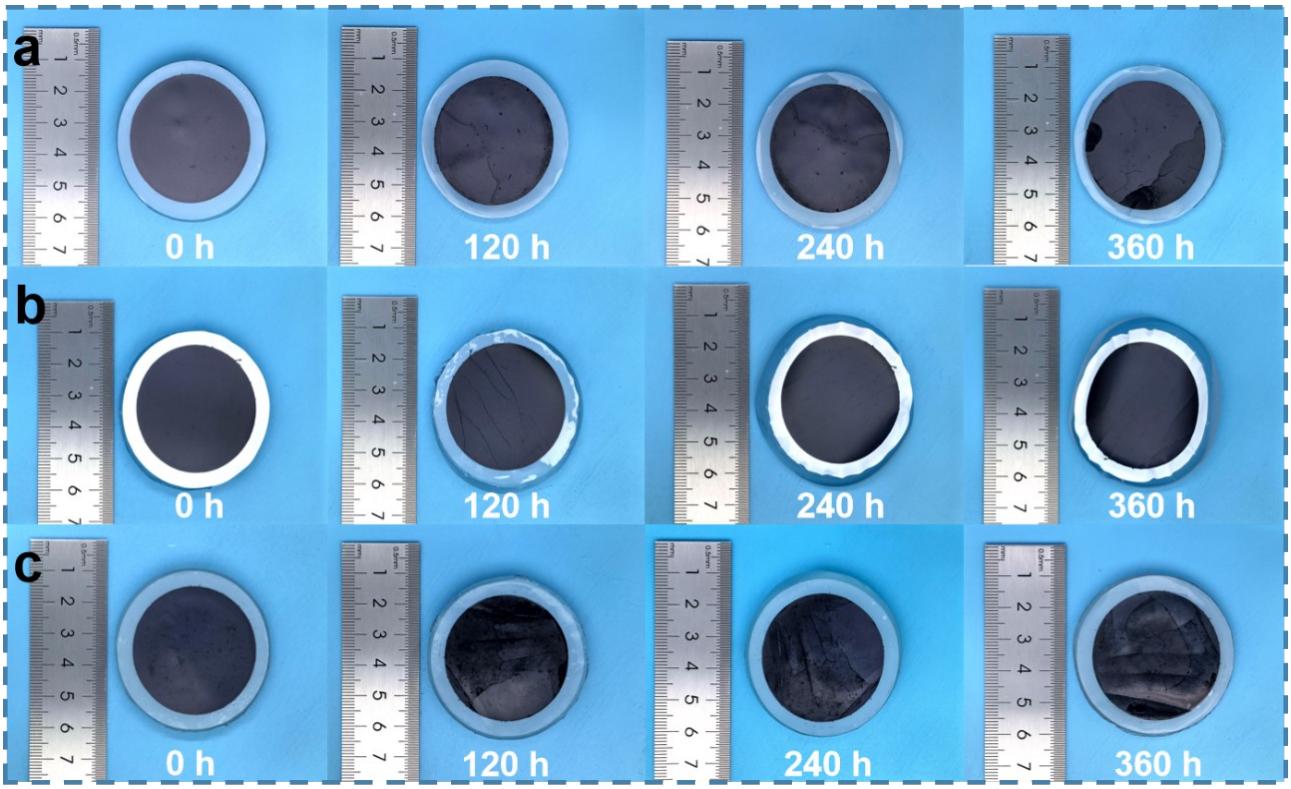

Figure S15 Long-term evaporation top-view of (a) MCH, (b) MPH and (c) MCPH evaporator surfaces in simulated seawater for 360 hours.

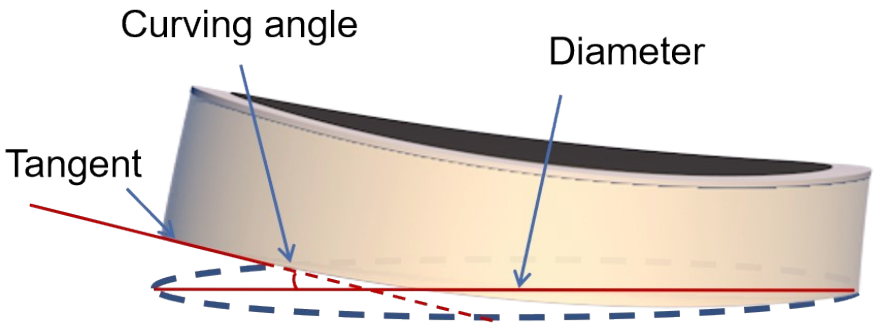

Figure S16 Diagram of curving angle.

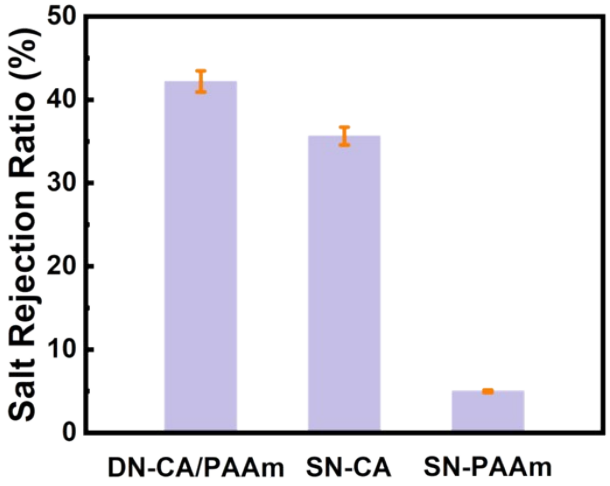

Figure S17 Salt-rejection ratio for SN-CA, SN-PAAm and DN-CA/PAAm hydrogels.

Additionally, the salt resistance of the MCPH evaporator was assessed (Fig. S17†). The results showed that both MCH and MCPH evaporators exhibit salt resistance, whereas the MPH evaporator does not. This difference is likely due to the incorporation of K^+ into the CA network during synthesis, which induces the Donnan effect. Overall, the MCPH evaporator demonstrates strong potential for desalination applications.

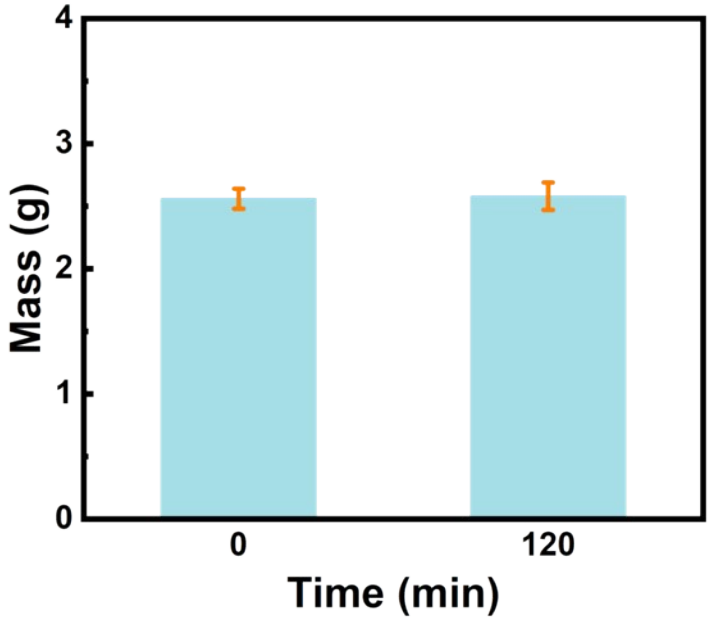

Figure S18 Mass of SN-CA hydrogels after 120 min immersion in water at 60℃.

Table S1 The evaporation efficiency of different evaporators.

Vapor	Evaporation Rate ($kg\ m^{-2}\ h^{-1}$)	Energy Effiency	Ref.
salt-free Janus steam generator	1.71	89.6%	[S2]
PDMS/CNT-PNIPAM sponge	1.66	99.9	[S3]
Ni_5P_4-$NiMoO_x$ (P-NMO)	1.49	93.0%	[S4]
polypyrrole-modified polyimide nanofiber aerogel (PPy-PI NAG)	1.42	95.8%	[S5]
Multifunctional hydrophilic MXene/Gelatin composite aerogel	1.70	90.3%	[S6]
zeolite-chitosan-TiO_2@PPy aerogel	1.66		[S7]
$Sr_{2.7}Ln_{0.3}Fe_{1.4}Co_{0.6}O_{7-\delta}$ (Ln = La or Nd) perovskites	1.67	95.0%	[S8]
A loofah-based photothermal biomass material	1.57	95.5%	[S9]
pulp-natural rubber (PNR)	1.62	98.1%	[S10]
Recyclable Monolithic Vitrimer Foam	1.35	89.2%	[S11]
Oxygen-Deficient MoO_{3-x}-rGO Composites	1.58	87.2%	[S12]
CPDH	1.78	91.2%	This work

References

[S1]Tao P., Ni G., Song C. Y., Shang W., Wu J. B., Zhu J., Chen G., Deng T, *Nat. Energy*, 2018, 3 , 1031-1041.

[S2]F. Wang, C. Wang, G. Shi, Y. Wang, F. Li, K. Xu, M. Ma, *Desalination*, 2023, 545, 116157.

[S3]Y. Cai, Y. Dong, K. Wang, D. Tian, J. Qu, J. Hu, J. Lee, J. Li, K.H. Kim, *J. Colloid Interface Sci.*, 2023, 629, 895-907.

[S4]L. Ai, Y. Xu, S. Qin, Y. Luo, W. Wei, X. Wang, J. Jiang, *J. Colloid Interface Sci.*, 2023, 634, 22-31.

[S5]T. Xue, F. Yang, X. Zhao, F. He, Z. Wang, Q. Wali, W. Fan, T. Liu, *Chem. Eng. J.*, 2023, 461, 141909.

[S6]N. Xue, H. Cui, W. Dong, W. Chu, M. Li, H. Jiang, N. Wei, *Chem. Eng. J.*, 2023, 455, 140614.

[S7]S. Zhao, X. Zhang, G. Wei, Z. Su, *Chem. Eng. J.*, 2023, 458, 141520.

[S8]E. Valadez-Renteria, J. Oliva, K.P. Padmasree, V. Rodriguez-Gonzalez, *Chem. Eng. J.*, 2023, 460, 141763.

[S9]X. Jia, X. Liu, H. Guan, T. Fan, Y. Chen, Y.-Z. Long, *Compos. Commun.*, 2023, 37, 101430.

[S10] Y. Zhang, W. Deng, M. Wu, Z. Liu, G. Yu, Q. Cui, C. Liu, P. Fatehi, B. Li, *ACS Appl. Mater. Interfaces*, 2023, 15, 7414-7426.

[S11] Y. Wang, W. Li, Y. Wei, Q. Chen, *ACS Appl. Mater. Interfaces*, 2023, 15, 14379-14387.

[S12] Y. Sun, S. Qiu, Z. Fang, J. Yang, X. Song, S. Xiao, *ACS Sustain. Chem. Eng.*, 2023, 11, 3359-3369.